World Journal of Surgical Oncology

RESEARCH

Open Access

Tertiary lymphoid structures' pattern and prognostic value in primary adenocarcinoma of jejunum and ileum

Minying Deng[1†], Xin Liu[2†], Yan Jiang[1†], Rongkui Luo[1], Lei Xu[1], Xiaolei Zhang[1], Jieakesu Su[1], Chen Xu[1*] and Yingyong Hou[1*]

Abstract

To date, there have been no reports on tertiary lymphoid structures (TLS) in primary adenocarcinoma of jejunum and ileum. In this study, we employed digital pathology image analysis software to classify and quantify TLS, and evaluated the maturity of TLS using immunohistochemistry. Molecular genetics and immunotherapy biomarker detection were performed using next-generation sequencing technology, such as tumor mutational burden (TMB) and microsatellite instability (MSI). The aim of this study was to investigate the presence, location, maturity, association with immunotherapy biomarkers, and prognostic value of TLS in primary adenocarcinoma of jejunum and ileum. Compared to secondary follicle-like TLS (SFL-TLS), intra-tumoral TLS (IT-TLS) were more likely to manifest as early TLS (E-TLS) ($P=0.007$). Compared to IT-TLS, SFL-TLS had a higher propensity to occur at the invasive margin (IM) ($P=0.032$) and showed a trend towards being more prevalent at the tumor periphery ($P=0.057$). In terms of immunotherapy biomarkers, there was a higher trend of IM-TLS density in PD-L1(22C3) score CPS < 1 group compared to PD-L1(22C3) score CPS ≥ 1 group ($P=0.071$). TMB-H was significantly associated with MSI-H ($P=0.040$). Univariate survival analysis demonstrated a correlation between high SFL-TLS group and prolonged disease free survival (DFS) ($P=0.047$). There was also a trend towards prolonged DFS in the E-TLS-high group compared to the E-TLS-low group ($P=0.069$). The peri-tumoral TLS (PT-TLS)-high group showed a trend of prolonged overall survival (OS) compared to the PT-TLS-low group ($P=0.090$). In conclusion, the majority of TLS were located at the invasive margin and tumor periphery, predominantly consisting of mature TLS, while IT-TLS were mainly immature. Notably, TMB was closely associated with MSI and PD-L1, indicating potential predictive value for immunotherapy in primary adenocarcinoma of jejunum and ileum.

Keywords Primary adenocarcinoma of jejunum and ileum, TLS, PD-L1, MSI, TMB

†Minying Deng, Xin Liu and Yan Jiang contributed equally to this work.

*Correspondence:
Chen Xu
xu.chen@zs-hospital.sh.cn
Yingyong Hou
hou.yingyong@zs-hospital.sh.cn
[1]Department of Pathology, Zhongshan Hospital, Fudan University, Shanghai 200032, China
[2]Department of Pathology, Eye & ENT Hospital, Fudan University, Shanghai 200032, China

Introduction

It is well-known that diagnosing and treating primary adenocarcinoma of jejunum and ileum is relatively challenging due to its location deep in the abdomen and often subtle early symptoms, which can lead to late detection or misdiagnosis. As a rare tumor, it has not been extensively studied in past research and is often managed with treatments used for colorectal or gastric cancers, such as oxaliplatin-based chemotherapy combined with fluoropyrimidines, or regimens like FOLFOX, CAPOX, and CAPIRINOX with or without bevacizumab. Despite these approaches, the prognosis of primary adenocarcinoma of jejunum and ileum remains poor, with a median overall survival (OS) of approximately 15.9 months [1].

In recent years, immunotherapy strategies targeting the tumor microenvironment have become a research focus, aiming to inhibit tumor growth and metastasis by activating immune cells, modulating cytokines, and altering the tumor microenvironment. Several solid tumors, such as gastric cancer and breast cancer, have shown favorable responses to immunotherapy [2, 3]. Tertiary lymphoid structures (TLS) are an integral part of the tumor microenvironment and represent ectopic lymphoid organs that develop within chronic inflammatory sites, including tumors. Anatomically, TLS resemble secondary lymphoid organs (SLO) and can induce delayed immune responses in the body. Previous studies have found a correlation between high-density TLS and better clinical outcomes in non-small cell lung cancer, malignant melanoma, pancreatic cancer, and esophageal cancer, among others [4–7]. However, the biological functions of TLS in primary adenocarcinoma of jejunum and ileum are not well understood and warrant further investigation.

It is well known that the discovery of PD-1 checkpoint inhibitors has revealed the mystery of how malignant tumors evade immune surveillance through interaction with their major ligand PD-L1. Blocking the interaction between the PD-1 receptor and PD-L1 has proven to have significant anticancer effects in some solid tumors [8]. However, many advanced tumors still show no response. Consequently, the US Food and Drug Administration (FDA) has approved the assessment of PD-L1 expression status, tumor mutational burden (TMB), and microsatellite instability (MSI) status as companion diagnostic biomarkers to guide PD-1 therapy. Nevertheless, not all tumor types can be predicted and scored uniformly, and individual assessment may be necessary depending on the specific tumor type [9]. Therefore, this study attempts to evaluate the spatial distribution, density, maximum diameter, and maturity of TLS in primary adenocarcinoma of jejunum and ileum in a more accurate and quantitative manner. Additionally, we aim to investigate the expression of PD-L1, MSI status, and TMB in primary adenocarcinoma of jejunum and ileum using immunohistochemistry and next-generation sequencing technology, respectively. The study aims to explore the interactions between these markers and their prognostic value in primary adenocarcinoma of jejunum and ileum, providing data support and reference for the treatment of this rare and highly malignant tumor.

Materials and methods

Study design and study population

This study is a single-center, non-interventional retrospective cohort study. The study population includes patients with primary adenocarcinoma of jejunum and ileum who underwent curative or partial small bowel resection at Zhongshan Hospital, Fudan University, between January 2014 and December 2023, and confirmed by histopathological diagnosis. Patients with duodenal adenocarcinoma were excluded. Patients with incomplete electronic medical records, incomplete follow-up data, histopathological confirmation of non-adenocarcinoma components or non-primary adenocarcinoma, preoperative neoadjuvant therapy such as chemotherapy, targeted therapy, radiation therapy, or immunotherapy, death within 30 days after surgery, or presence of dual or multiple primary tumors were also excluded. Additionally, tumor samples must be paired with adjacent non-tumor tissue. Tumor samples without adjacent normal tissue were excluded from the study. Clinical and pathological parameters were retrospectively collected from the hospital's medical records database, including initial diagnosis age, gender, pathological characteristics, lymph node metastasis, TNM staging, surgical history, and other relevant factors.

Follow-up started on the day of surgery and continued until December 2023. Patients were followed up every 3 months in the first year after surgery and every 6 months in the second and third years. Electronic medical records and telephone interviews were conducted to record the relationship between the respondent and the patient, patient cooperation, brief medical history, survival status, tumor recurrence, abdominal ultrasonography, colonoscopy, abdominal CT scans, etc. OS was defined as the time from the day of surgery to the occurrence of an event (death) or the last follow-up. This study was approved by the Ethics Committee of Zhongshan Hospital, Fudan University (Ethics Approval No: B2023-304R).

Hematoxylin & Eosin (H&E) and immunohistochemical staining

Two experienced pathologists independently reviewed slides according to the routine protocol in the department of pathology and evaluated the presence of adenocarcinoma tissue and adjacent normal intestinal mucosal tissue on the slides. Formalin-fixed paraffin-embedded (FFPE) samples included in this study were retrieved

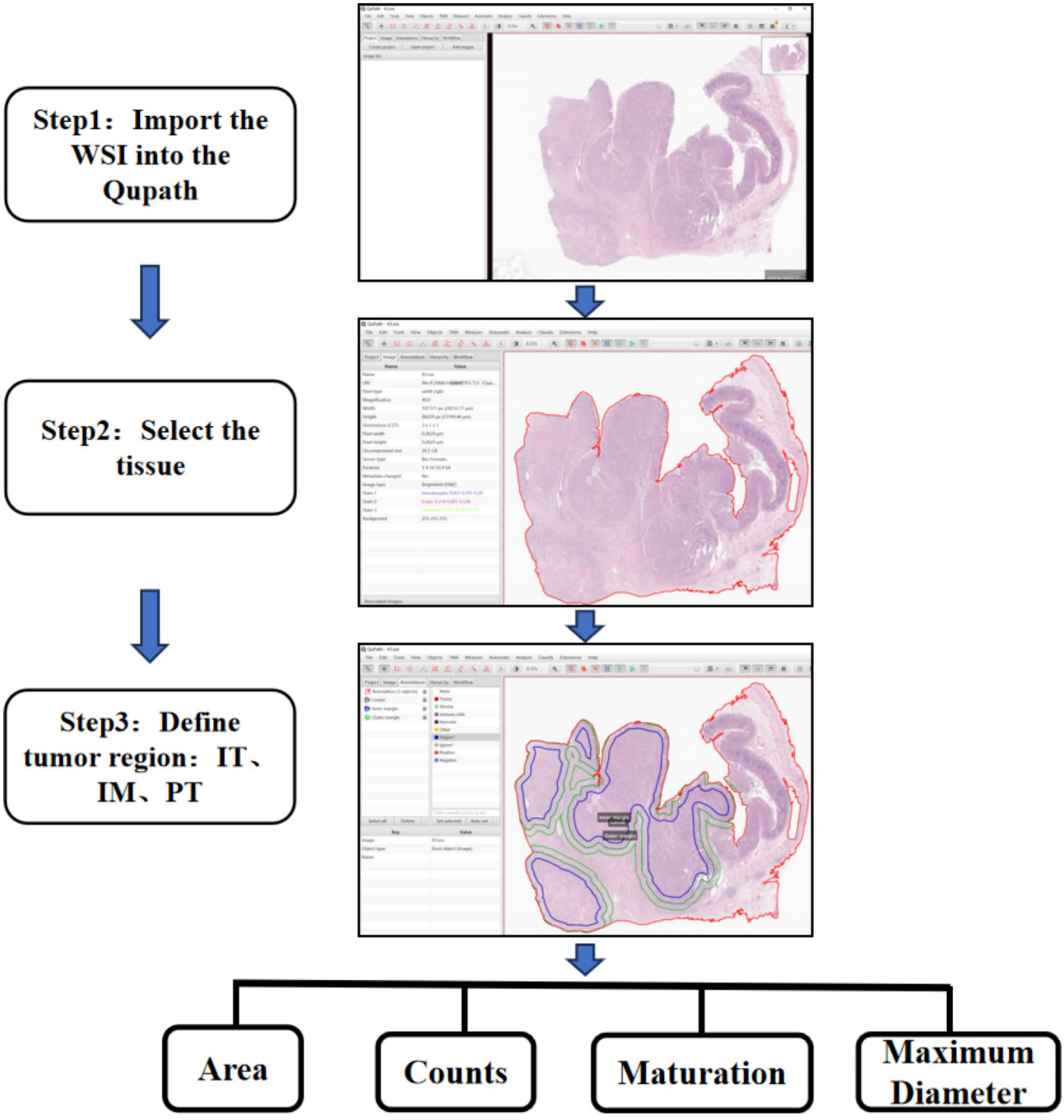

Fig. 1 Flow chart of spatial partitioning and maturity assessment of TLS using digital pathology image analysis software

and processed to obtain 4 μm thick sections. The sections were deparaffinized, hydrated, stained with H&E, differentiated, counterstained, dehydrated, and air-dried using standard procedures. Neutral mounting medium was used for coverslipping, and the slides were observed under a light microscope. Immunohistochemistry was optimized to obtain the best platform conditions and concentrations for this study through multiple trials and adjustments. Immunohistochemical staining was performed using the EnVision two-step method. Immunostaining for CD4, CD8, CD20, CD56, CD21, CD23 and PD-L1 was carried out using the Leica ST5020 multiple staining system (Leica Biosystems). The primary antibodies were anti-CD4 (1:3000 dilution, clone EP204, Genetech) mouse monoclonal antibody, anti-CD8 (1:300 dilution, clone 4B11, LEICA) rabbit monoclonal antibody, anti-CD20 (1:4 dilution, clone L26, DAKO) mouse monoclonal antibody, anti-CD56 (1:100 dilution, clone

1B6, LEICA) mouse monoclonal antibody, anti-CD21 (1:100 dilution, clone 2G9, LEICA) mouse monoclonal antibody, anti-CD23 (1:600 dilution, clone DAK-CD23, DAKO) mouse monoclonal antibody, and anti-PD-L1 (1:4 dilution, clone 22C3, DAKO) mouse monoclonal antibody. Immunohistochemical staining was performed according to the manufacturer's instructions, with positive and negative controls set up as routine. All immunohistochemical staining was performed on tissue microarray sections to avoid heterogeneity and the omission of TLS assessment. The above-mentioned slides were scanned using the Leica Aperio GT450 scanner to obtain high-resolution whole slide images (WSI).

Pathological assessment of TLS

For each case in the cohort, slides were independently evaluated by two pathologists who were unaware of the specific clinical history and relevant information of the patients. As mentioned earlier, TLS were morphologically assessed on H&E-stained slides. Tumor TLS are aggregates of tumor-infiltrating lymphocytes (TILs) at sites of chronic inflammatory stimulation within the tumor, characterized by a central area of CD20+B cells surrounded by CD3+T cells [10]. Following the literature, the minimum diameter of TLS was defined as 150 μm in this study [11]. To evaluate the spatial distribution and locational heterogeneity of TLS, all WSIs were imported into the digital pathology image analysis software Qupath (version 0.5.1), and all WSIs were divided into three subregions: intra-tumoral (IT), infiltrative margin (IM, defined as the tissue area from the boundary between the host tissue and the malignant tumor nests outward, with a range of 500 μm), and peri-tumoral (PT) [12, 13]. To determine the maturity of TLS in primary adenocarcinoma of jejunum and ileum, immunohistochemical staining was performed on consecutive sections of the same sample, and the staining intensity and extent of CD4+T cells, CD8+T cells, CD20+B cells, CD56+NK cells, CD21+follicular dendritic cells (FDCs), and CD23+germinal center (GC) cells within TLS were evaluated. Based on the maturity stage, TLS were classified into the following stages: (1) early TLS (E-TLS), characterized by a mixed distribution of T cells and B cells in lymphocytic aggregates but lacking CD21+FDCs and CD23+GC components; (2) primary follicle-like TLS (PFL-TLS), consisting of follicle-like structures formed by B cells at the center, surrounded by T cells and a small number of CD21+FDCs but lacking CD23+GC; and (3) secondary follicle-like TLS (SFL-TLS), which represents the appearance of lymph node-like CD23+GC components within PFL-TLS, manifesting as a lightly stained area within the central area of lymphocytic aggregates on H&E slides [14–17]. In this study, the area of intratumoral, infiltrative margin, and peri-tumoral regions was evaluated using the Qupath software. The number of TLS at each maturity stage was calculated, and TLS density was determined by calculating the number of TLS per square millimeter within the target area. The maximum diameter of TLS at each maturity stage was also measured (Fig. 1).

PD-L1 immunohistochemistry assessment

To accurately detect the expression levels of PD-L1 in primary adenocarcinoma of jejunum and ileum, immunohistochemical staining with PD-L1 (22C3) was performed and interpreted. The comprehensive positive score (CPS) was used to evaluate the expression levels of PD-L1 protein in tumor cells and immune cells: CPS = (the number of PD-L1-positive tumor cells, lymphocytes, and macrophages)/(the total number of tumor cells) × 100. PD-L1 expression is considered positive when CPS ≥ 1. The tumor proportion score (TPS) was used to assess the expression levels of PD-L1 protein in tumor tissue: TPS = (the number of PD-L1-positive tumor cells)/(the total number of tumor cells) × 100%. PD-L1 is considered positive when TPS ≥ 1% [18, 19].

TMB and MSI status assessment

We retrospectively reviewed the electronic medical records of primary adenocarcinoma of jejunum and ileum patients who underwent next-generation sequencing analysis at our center. DNA was extracted from FFPE samples with at least 40% tumor content according to the instructions of the nucleic acid extraction kit (Aidlab, version B4.1). Next-generation sequencing was performed using the Illumina Novaseq 6000/Nextseq platform with hybrid capture-based targeted enrichment. TMB was defined as the total number of base substitution mutations and indel mutations per megabase (Mb) of the tumor genome, with a unit of muts/Mb. We defined TMB values ≥ 10 muts/Mb as TMB-H and < 10 muts/Mb as TMB-L. The Master Panel project in this study included 116 microsatellite candidate loci, and based on the status of repeat base changes at each locus, the loci were classified as microsatellite stable (MSS) or MSI. When the proportion of MSI loci was ≥ 15%, the MSI test result was considered positive, indicating MSI-H.

Statistical analysis

Statistical and graphical analyses were performed using SPSS 25.0 (IBM, China) and GraphPad Prism Version 9.5.1 (733). One-way analysis of variance (ANOVA) was used to compare continuous variables among multiple groups (≥ 2), and Student's t-test was used to assess continuous variables between two groups. Categorical variables were analyzed using the chi-square test or Fisher's exact test. Kaplan-Meier survival curves and the log-rank test were used to evaluate differences in survival rates.

Cox proportional hazards regression analysis was performed to determine independent prognostic factors for disease free survival (DFS) and OS, with variables significantly associated with DFS or OS in univariate analysis included in the multivariate analysis. All hypothesis tests were two-sided, and a P-value < 0.05 was considered statistically significant. P-values between 0.05 and 0.1 were considered indicative of a trend.

Results

Clinical and pathological characteristics

Table 1 summarizes the clinical and pathological characteristics of the patients in this study cohort. In this study cohort, the 1-year, 3-year, and 5-year survival rates were 95.6%, 73.2%, and 7.5%, respectively. The 1-year, 3-year, and 5-year recurrence/metastasis rates were 13.0%, 22.2%, and 25.9%, respectively. More than half of the patients were male (55.6%). The median age was 59 years (range 27–85 years). The median maximum diameter of the tumor was 3.5 cm (range 1–12 cm). The most common site of origin was the jejunum (70.4%). Lymphatic invasion was observed in 27 cases (50%), vascular invasion in 19 cases (35.2%), neural invasion in 36 cases (66.7%), lymph node metastasis in 14 cases (25.9%), and tumor nodules in 15 cases (27.8%). According to the UICC/AJCC TNM staging criteria, there were 24 cases (44.4%) in stage II, 6 cases (11.1%) in stage III, and 24 cases (44.4%) in stage IV. As of December 2023, the average follow-up time for this cohort was 24.6 months, with a median follow-up time of 15 months. The median DFS was 7 months (range 0–82 months), and the median OS was 15 months (range 1-100 months).

Heterogeneous characteristics of TLS localization in primary adenocarcinoma of jejunum and ileum

The presence, spatial distribution (intra-tumoral, infiltrative margin, or peri-tumoral), and maturity stage (E-TLS, PFL-TLS, or SFL-TLS) of TLS were initially assessed based on H&E-stained slides from 54 patients. Within this cohort, TLS were identified in approximately 33 cases (61.1%). Regarding spatial distribution, IT-TLS were present in 31 cases (57.4%), IM-TLS in 30 cases (55.6%), and PT-TLS in 32 cases (59.3%). The median number of IT-TLS was 5 (range 1–34), with a median maximum diameter of 581 μm (range 157–1467 μm). For IM-TLS, the median number was 5 (range 1–28), with a median maximum diameter of 582 μm (range 229–1718 μm). PT-TLS had a median number of 6 (range 1–54) and a median maximum diameter of 661 μm (range 208–1514 μm). We found that TLS varied in size and shape, with TLS located in the small intestinal mucosa often being flattened and elongated or teardrop-shaped, while those in the submucosa and muscularis propria were typically oval-shaped. TLS were predominantly covered by CD20+B lymphocytes, and CD4+T lymphocytes and CD8+T lymphocytes were mainly located in T-cell areas. IT-TLS, IM-TLS, and PT-TLS all demonstrate that TLS are predominantly comprised of CD20+B lymphocytes, with relatively fewer CD4+T lymphocytes and CD8+T lymphocytes present. Foxp3+T regulatory cells and CD56 + NK cells are relatively rare within TLS. Compared to PT-TLS, IT-TLS and IM-TLS exhibit a higher number of CD8+T cells, with statistical significance (P<0.05). However, there is no significant difference in the quantity of CD20+B cells, CD4+T cells, Foxp3+Treg cells and CD56+NK cells among IT-TLS, IM-TLS, and PT-TLS (Figs. 2 and 3).

Heterogeneous characteristics of TLS maturity in primary adenocarcinoma of jejunum and ileum

To investigate the maturity of TLS in primary adenocarcinoma of jejunum and ileum, we performed consecutive sections on samples with TLS structures on H&E slides and evaluated the staining intensity and extent of CD4+T cells, CD8+T cells, CD20+B cells, CD56+NK cells, CD21+FDCs, and CD23+GC cells within TLS. The median total number of TLS was 24 (range 5–76), with a median of 7 E-TLS (range 0–54), 4 PFL-TLS (0–37), and 5 SFL-TLS (range 0–50). Statistical analysis showed no significant difference in the number of TLS among intratumoral, infiltrative margin, and peri-tumoral regions (P=0.7931). However, the density of TLS in the infiltrative margin was significantly higher than that in the intra-tumoral (P<0.0001) and peri-tumoral (P<0.0001) regions, with significant differences. There was a trend of larger maximum diameter of PT-TLS compared to IT-TLS and IM-TLS (P=0.0710). When evaluating the maturity of TLS in all included samples, it was found that E-TLS was the predominant component in primary adenocarcinoma of jejunum and ileum, followed by SFL-TLS, and PFL-TLS had a slightly lower proportion, but there was no significant difference among the three (P=0.2150). To explore the impact of TLS localization heterogeneity on TLS maturity and further investigate the heterogeneity of TLS components in different locations, we evaluated TLS with different spatial distributions. The results showed that IT-TLS were more likely to have E-TLS compared to SFL-TLS (P=0.007); the frequency of E-TLS was also relatively higher compared to PFL-TLS, but there was no significant difference (P=0.2441). For IM-TLS and PT-TLS, there were no significant differences in the distribution of E-TLS, PFL-TLS, and SFL-TLS (P=0.2964, P=0.1426). In terms of the maturity of TLS in different locations, this study also compared them. Compared to IT-TLS, SFL-TLS were more likely to occur in the infiltrative margin (P=0.0320), with a trend of being more common in the peri-tumoral region (P=0.0565). However, there were no significant

Table 1 Relationship among TLS, PD-L1(22C3) and clinical pathological features in 33 patients with TLS + primary adenocarcinoma of jejunum and ileum

Clinical pathological features		Cases	TLS density		*P* value	IT-TLS density		*P* value	IM-TLS density		*P* value	PT-TLS density		*P* value	E-TLS density		*P* value	PEL-TLS density		*P* value	SFL-TLS density		*P* value
			High	Low		High	Low		High	Low		High	Low		High	Low		High	Low		High	Low	
Age(y)	≤60	20	11	9	0.728	11	9	0.728	12	8	0.276	11	9	0.728	9	11	0.481	10	10	1.000	12	8	0.296
	>60	13	6	7		6	7		5	8		6	7		8	5		7	6		5	8	
sex	M	19	10	9	1.000	8	11	0.296	9	10	0.728	11	8	0.491	9	10	0.728	10	9	1.000	11	8	0.491
	F	14	7	7		9	5		8	6		6	8		8	6		7	7		6	8	
Tumor site	Jejunum	27	15	12	0.398	14	13	1.000	15	12	0.398	15	12	0.398	15	12	0.398	14	13	1.000	12	15	0.175
	Ileum	6	2	4		3	3		2	4		2	4		2	4		3	3		5	1	
Tumor size(cm)	≤5	23	12	11	1.000	13	10	0.465	12	11	1.000	10	13	0.259	13	10	0.465	14	9	0.141	10	13	0.259
	>5	10	5	5		4	6		5	5		7	3		4	6		3	7		7	3	
Macroscopic tumor perforation	Yes	2	1	1	1.000	2	0	0.485	1	1	1.000	1	1	1.000	2	0	0.485	0	2	0.227	0	2	0.227
	No	31	16	15		15	16		16	15		16	15		15	16		17	14		17	14	
Differentiation grade	Moderately differentiation	22	12	10	1.000	13	9	0.698	12	10	1.000	12	10	0.682	11	11	1.000	12	10	0.682	12	10	0.682
	Poorly differentiation	8	4	4		4	4		4	4		3	5		4	4		3	5		3	8	
Lymphatic invasion	Yes	21	9	12	0.282	11	10	1.000	11	10	1.000	10	11	0.721	11	10	1.000	10	11	0.721	11	10	1.000
	No	12	8	4		6	6		6	6		7	5		6	6		7	5		6	6	
Vascular invasion	Yes	10	3	7	0.141	3	7	0.141	4	6	0.465	3	7	0.141	4	6	0.465	5	5	1.000	5	5	1.000
	No	23	14	9		14	9		13	10		14	9		13	10		12	11		12	11	
Neural invasion	Yes	22	10	12	0.465	12	10	0.727	13	9	0.282	11	11	1.000	11	11	1.000	13	9	0.282	10	12	0.465
	No	11	7	4		5	6		4	7		6	5		6	5		4	7		7	4	
Tumor nodules	Yes	11	4	7	0.282	3	8	0.071	4	7	0.282	3	8	0.071	6	5	1.000	5	6	0.721	6	5	1.000
	No	22	13	9		14	8		13	9		14	8		11	11		12	10		11	11	
Mucinous component	Yes	7	2	5	0.225	1	6	0.039	2	5	0.225	3	4	0.688	4	3	1.000	4	3	1.000	4	3	1.000
	No	26	15	11		16	10		15	11		14	12		13	13		13	13		13	13	
T stage	T3	12	9	3	0.071	8	4	0.282	7	5	0.721	7	5	0.721	7	5	0.721	4	8	0.157	6	6	1.000
	T4	21	8	13		9	12		10	11		10	11		10	11		13	8		11	10	
N stage	N0	22	12	10	0.721	12	10	0.721	13	9	0.282	13	9	0.282	12	10	0.721	12	10	0.721	11	11	1.000
	N1-3	11	5	6		5	6		4	7		4	7		5	6		5	6		6	5	
M stage	M0	16	10	6	0.303	8	8	1.000	8	8	1.000	11	5	0.084	7	9	0.494	10	6	0.303	8	8	1.000
	M1	17	7	10		9	8		9	8		6	11		10	7		7	10		9	8	
TNM stage	II	12	7	5	0.721	6	6	1.000	7	5	0.721	8	4	0.282	6	6	1.000	7	5	0.721	6	6	1.000
	III-IV	21	10	11		11	10		10	11		9	12		11	10		10	11		11	10	
PD-L1(22C3)	CPS ≥ 1	11	6	5	1.000	5	6	0.721	3	8	0.071	8	3	0.141	4	7	0.282	7	4	0.465	6	5	1.000
	CPS<1	22	11	11		12	10		14	8		9	13		13	9		10	12		11	11	
MSI-H	Yes	3	2	1	1.000	1	2	0.601	15	15	1.000	2	1	1.000	1	2	0.601	1	2	0.601	2	1	1.000
	No	30	15	15		16	14		2	1		15	15		16	14		16	14		15	15	

Table 1 (continued)

Clinical pathological features		Cases	TLS density		*P* value	IT-TLS density		*P* value	IM-TLS density		*P* value	PT-TLS density		*P* value	E-TLS density		*P* value	PEL-TLS density		*P* value	SFL-TLS density		*P* value
			High	Low		High	Low		High	Low		High	Low		High	Low		High	Low		High	Low	
TMB	High	12	9	3	0.073	6	6	1.000	6	6	1.000	8	4	0.282	5	7	0.481	7	5	0.721	6	6	1.000
	Low	21	8	13		11	10		11	10		9	12		12	9		10	11		11	10	
KRAS mutation	Yes	17	9	8	1.000	9	8	1.000	11	6	0.169	10	7	0.494	10	7	0.494	10	7	0.494	8	9	0.732
	No	16	8	8		8	8		6	10		7	9		7	9		7	9		9	7	
BRAF mutation	Yes	31	16	15	1.000	15	16	0.485	17	14	0.227	16	15	1.000	16	15	1.000	16	15	1.000	16	15	1.000
	No	2	1	1		2	0		0	2		1	1		1	1		1	1		1	1	
PIK3CA mutation	Yes	1	1	0	1.000	1	0	1.000	1	0	0.515	1	0	1.000	0	1	0.485	0	1	0.485	1	0	1.000
	No	32	16	16		16	16		16	16		16	16		17	15		17	15		16	16	

differences in the distribution of E-TLS ($P=0.2003$) and PFL-TLS ($P=0.3434$) among the three spatial locations (Figs. 4, 5, 6 and 7).

Relationship between TLS spatial localization, maturity, and clinical pathological characteristics in primary adenocarcinoma of jejunum and ileum

According to the statistical results of TLS density and clinicopathological features, it suggests that high-density TLS group is associated with better clinicopathological characteristics, such as better differentiation, absence of lymph node metastasis, no neural invasion, no lymphatic invasion, no vascular invasion, no tumor nodules, no mucinous component, and lower T stage and TNM stage. However, currently, only T stage has been observed to have statistical significance. Compared to T4 stage, patients with T3 stage had a higher trend of TLS percentage (75.00% vs. 38.10%, $P=0.071$). There was no significant difference in TLS percentage between lymph node-negative and lymph node-positive patients (54.55% vs. 45.45%, $P=0.721$). There was no significant difference in TLS percentage between patients with or without neural invasion (45.45% vs. 63.64%, $P=0.465$). Similarly, there was no significant difference in TLS percentage between patients with or without lymphatic invasion (42.86% vs. 66.67%, $P=0.282$), vascular invasion (30.00% vs. 60.87%, $P=0.141$), tumor nodules (36.36% vs. 59.09%, $P=0.282$), mucinous component (28.57% vs. 57.69%, $P=0.225$), moderate or low differentiation (54.55% vs. 50%, $P=1.000$), or TNM stage II or III/IV (58.33% vs. 47.62%, $P=0.721$). Analysis based on spatial localization found that IT-TLS density was higher in the group without mucinous component (61.54% vs. 14.29%, $P=0.039$). Compared to the group with tumor nodules, there was a trend of higher IT-TLS density and PT-TLS density in the group without tumor nodules (27.27% vs. 63.64%, $P=0.071$). Similarly, compared to the M1 group, PT-TLS density showed a higher trend in the M0 group (35.29% vs. 68.75%, $P=0.084$). Furthermore, no statistical differences were observed between the maturity of TLS (E-TLS, PFL-TLS, SFL-TLS) and clinical pathological characteristics (Table 1).

Relationship between TLS spatial localization, maturity, and PD-L1, TMB, and other molecular features in primary adenocarcinoma of jejunum and ileum

We first analyzed the correlation between PD-L1 (22C3) expression levels and clinical pathological characteristics in this cohort. Among the 54 cases of primary adenocarcinoma of jejunum and ileum, compared to patients with CPS<1, those with CPS≥1 were more likely to have low differentiation and absence of mucinous component, showing a positive correlation ($P=0.013$, $P=0.037$). However, compared to the CPS≥1 group, the CPS<1

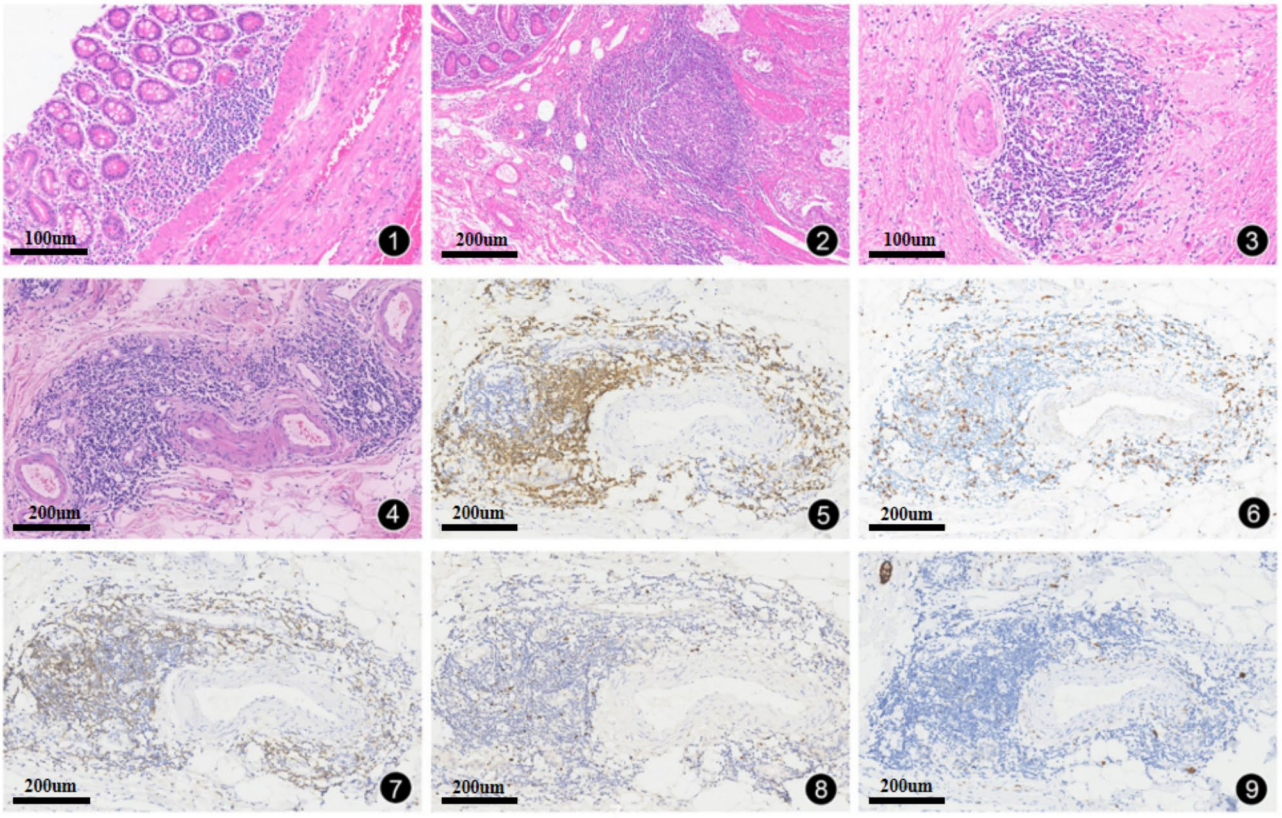

Fig. 2 TLS in primary adenocarcinoma of jejunum and ileum. (1) The mucosal TLS was flattened and elongated or teardrop-shaped; (2, 3) the submucosal and basal lamina propria TLS were typically oval-shape; (4) TLS in muscularis propria; (5) CD20 + B cells; (6) CD8 + T cells; (7) CD4 + T cells; (8) Foxp3 + Treg cells; (9)CD56 + NK cells. The scale bars on the H&E and immunohistochemical images indicate 100 μm (1, 3) and 200 μm (2,4–9)

group showed a positive correlation with neural invasion, distant metastasis (M1), and TNM stage ($P=0.014$, $P=0.020$, $P=0.007$) (Fig. 8).

Furthermore, we performed a stratified analysis specifically in the TLS + group. In this subgroup, we found that CPS ≥ 1 was positively correlated with the tumor maximum diameter ($P=0.049$). The association between CPS and neural invasion was consistent with the previous findings ($P=0.017$). There was a trend toward lower CPS scores in the moderately differentiated group compared to the poorly differentiated group ($P=0.078$). Notably, there was also a trend indicating higher IM-TLS density in the CPS < 1 group compared to the CPS ≥ 1 group (27.27% vs. 63.64%, $P=0.071$).

For the 54 cases of primary adenocarcinoma of jejunum and ileum, TMB was analyzed and classified into TMB-H group and TMB-L group. This study found a significant statistical difference between TMB-H and MSI-H ($P=0.004$), with TMB-H tumors more common in the jejunum (68.75% vs. 31.58%, $P=0.012$), and more likely to occur in patients without distant metastasis (M0) and TNM II-III stage ($P=0.019$, $P=0.022$). Compared to the CPS < 1 group, there was a trend of TMB-H tumors being more common in the CPS ≥ 1 group (33.33% vs. 61.11%, $P=0.052$).

In the analysis specifically for the TLS + group, it was also found that TMB-H was significantly positively correlated with MSI-H (100% vs. 30%, $P=0.040$). Compared to the lymphatic invasion-positive group, TMB-H tumors tended to be more common in the lymphatic invasion-negative group (23.81% vs. 58.33%, $P=0.067$). Compared to the TMB-L group, TMB-H tumors showed a trend of higher TLS density (38.10% vs. 75%, $P=0.073$).

Furthermore, in the 54 cases of primary adenocarcinoma of jejunum and ileum, this study also explored the relationship between the aforementioned indicators (such as the presence of TLS, PD-L1 (22C3), TMB, MSI, etc.) and mutations in *KRAS*, *NRAS*, *BRAF*, and *PIK3CA* genes. Compared to the TLS + group, the TLS- group showed a trend of higher frequency of *NRAS* gene mutations (0% vs. 9.52%, $P=0.073$). TMB-H tumors were more likely to occur in the non-*KRAS* gene mutation group, showing a statistically significant difference (58.33% vs. 30%, $P=0.036$). In the TLS + group, no significant statistical significance was found in the relationship between the aforementioned indicators (including TLS spatial

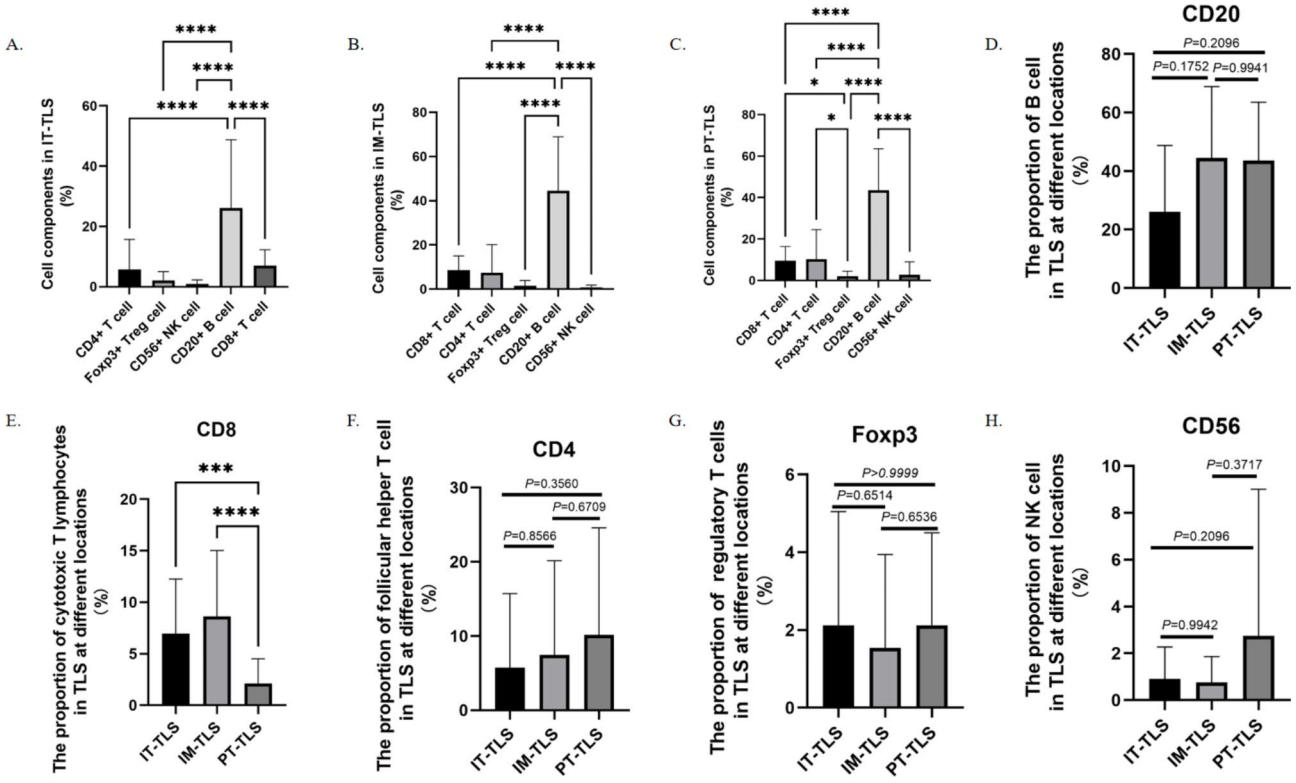

Fig. 3 Cellular composition of TLS. (**A**, **B**, **C**) IT-TLS, IM-TLS, and PT-TLS all demonstrate that TLS are predominantly comprised of CD20 + B lymphocytes, with relatively fewer CD4 + T lymphocytes and CD8 + T lymphocytes present. Foxp3 + T regulatory cells and NK cells are relatively rare within TLS. (**D**) There is no significant difference in the quantity of CD20 + B cells among IT-TLS, IM-TLS, and PT-TLS. (**E**) Compared to PT-TLS, IT-TLS and IM-TLS exhibit a higher number of CD8 + T cells, with statistical significance ($P < 0.05$). (**F**) There is no significant difference in the number of CD4 + T cells between IT-TLS, IM-TLS, and PT-TLS. (**G**) There is no significant difference in the number of Foxp3 + Treg cells among IT-TLS, IM-TLS, and PT-TLS. (**H**) There is no significant difference in the number of CD56 + NK cells between IT-TLS, IM-TLS, and PT-TLS

localization and maturity) and molecular alterations (Tables 2 and 3).

Relationship between TLS spatial localization, maturity, and other clinical pathological parameters and prognosis in primary adenocarcinoma of jejunum and ileum

Previous research has indicated that infiltrative margin is primarily composed of mature TLS, while IT-TLS is mainly composed of immature TLS. Therefore, the relationship between TLS maturity, spatial localization heterogeneity, and prognosis deserves further exploration. Univariate survival analyses revealed that the SFL-TLS-high group was associated with prolonged DFS ($P=0.047$), although there was no significant relationship with OS ($P=0.966$). Additionally, compared to the E-TLS-low group, the E-TLS-high group also demonstrated a trend of prolonged DFS ($P=0.069$), but no significant difference in OS was observed ($P=0.383$). In terms of spatial localization, compared to the PT-TLS-low group, the PT-TLS-high group showed a trend of prolonged OS ($P=0.090$). There were no significant statistical differences in TLS density at the invasive margins and intra-tumoral regions with respect to clinical progression or survival duration. In addition, in the TLS+group, univariate survival analysis showed that N stage (OS, $P<0.001$; DFS, $P<0.001$), M stage (OS, $P=0.044$; DFS, $P=0.001$), and TNM stage (OS, $P=0.077$; DFS, $P=0.011$) were associated with shorter OS and DFS. However, further multivariate Cox regression analysis revealed that none of these factors were independent prognostic factors (Table 4; Fig. 9).

Discussion

In the past decade, the field of immunotherapy has seen remarkable advancements, prompting extensive research into the immune microenvironment of various solid tumors. As an ectopic lymphoid organ, TLS have emerged as a focal point of this research due to their potential implications in cancer prognosis and therapy. Currently, numerous studies have found a positive correlation between TLS and favorable prognosis in various cancers, such as renal clear cell carcinoma, breast cancer, endometrial cancer, ovarian cancer, bladder cancer, lung cancer, colorectal cancer, soft tissue sarcoma, pancreatic neuroendocrine tumors, and malignant melanoma. Given the limited understanding of TLS's

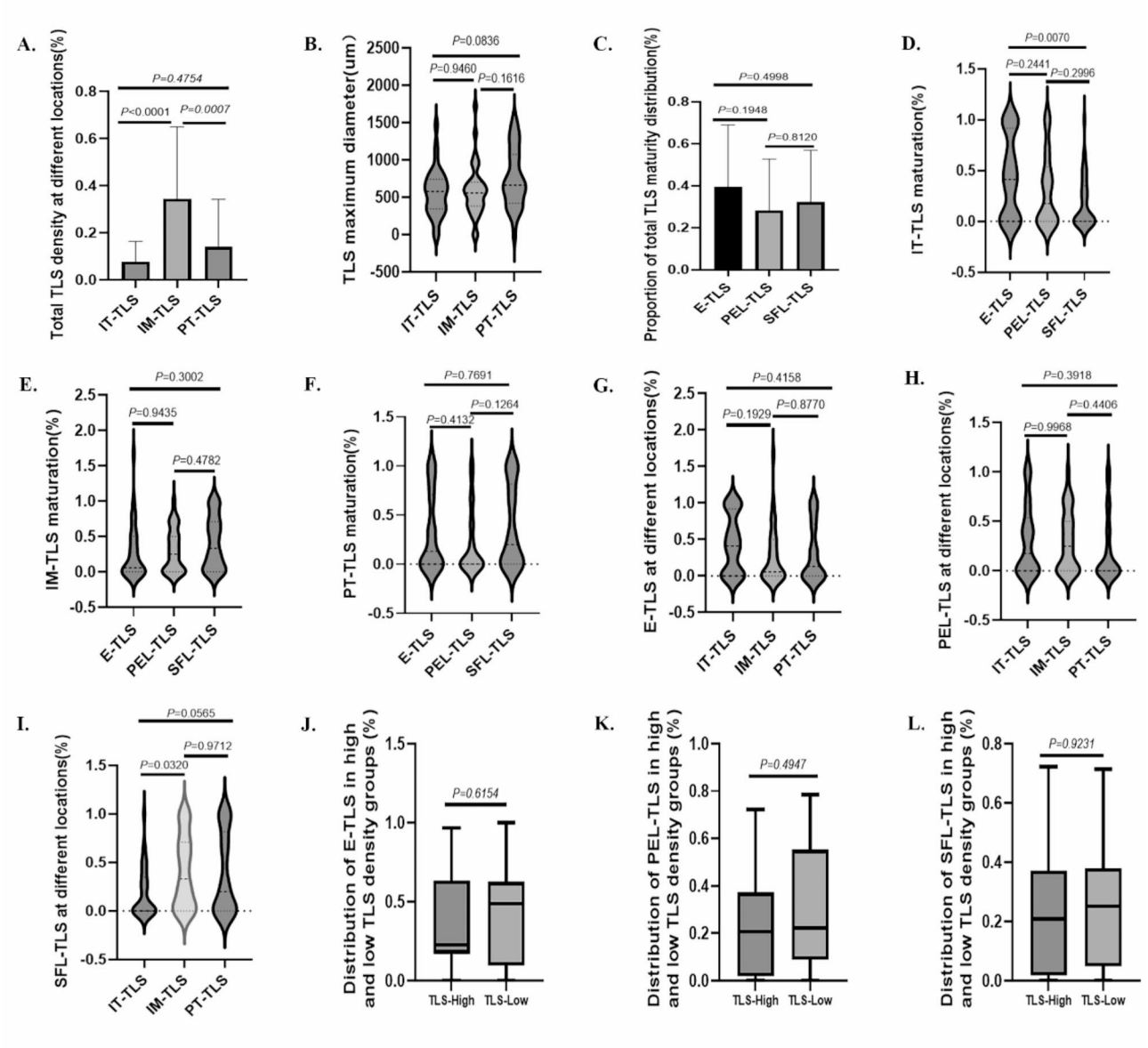

Fig. 4 Heterogeneous distribution of TLS spatial positioning and maturity in primary adenocarcinoma of jejunum and ileum. (**A**) TLS density in different locations; (**B**) Maximum diameter of TLS in different locations; (**C**) Heterogeneity of TLS maturity in different locations; (**D**) Maturity of IT-TLS; (**E**) Maturity of IM-TLS; (**F**) Maturity of PT-TLS; (**G**) Proportion of E-TLS in different locations; (**H**) Proportion of PEL-TLS in different locations; (**I**) Proportion of SFL-TLS in different locations; (**J**) Distribution of E-TLS in TLS-High and TLS-Low groups; (**K**) Distribution of PEL-TLS in TLS-High and TLS-Low groups; (**L**) Distribution of SFL-TLS in TLS-high and TLS-how groups

biological function in primary adenocarcinoma of jejunum and ileum, we aimed to clarify their impact by analyzing tumor data from 54 patients at our research center. Firstly, we examined the presence of TLS in the tumor, and if present, we used artificial intelligence software to determine the spatial localization and density of TLS, and employed immunohistochemical staining to evaluate the specific cell types and maturity of TLS. In addition, we employed next-generation sequencing to assess the MSI status and TMB, aiming to provide relevant information regarding the immune microenvironment of this tumor and the potential for immunotherapy.

To the best of our knowledge, this project represents the first study investigating the presence and prognostic significance of TLS in primary adenocarcinoma of jejunum and ileum. In our cohort, we found that 61.1% of the enrolled samples exhibited the presence of TLS. Specifically, among these samples, 57.4% contained IT-TLS, 55.6% exhibited IM-TLS, and 59.3% showed the presence of PT-TLS. These proportions are slightly lower than those reported in Wang et al.'s study in colorectal cancer

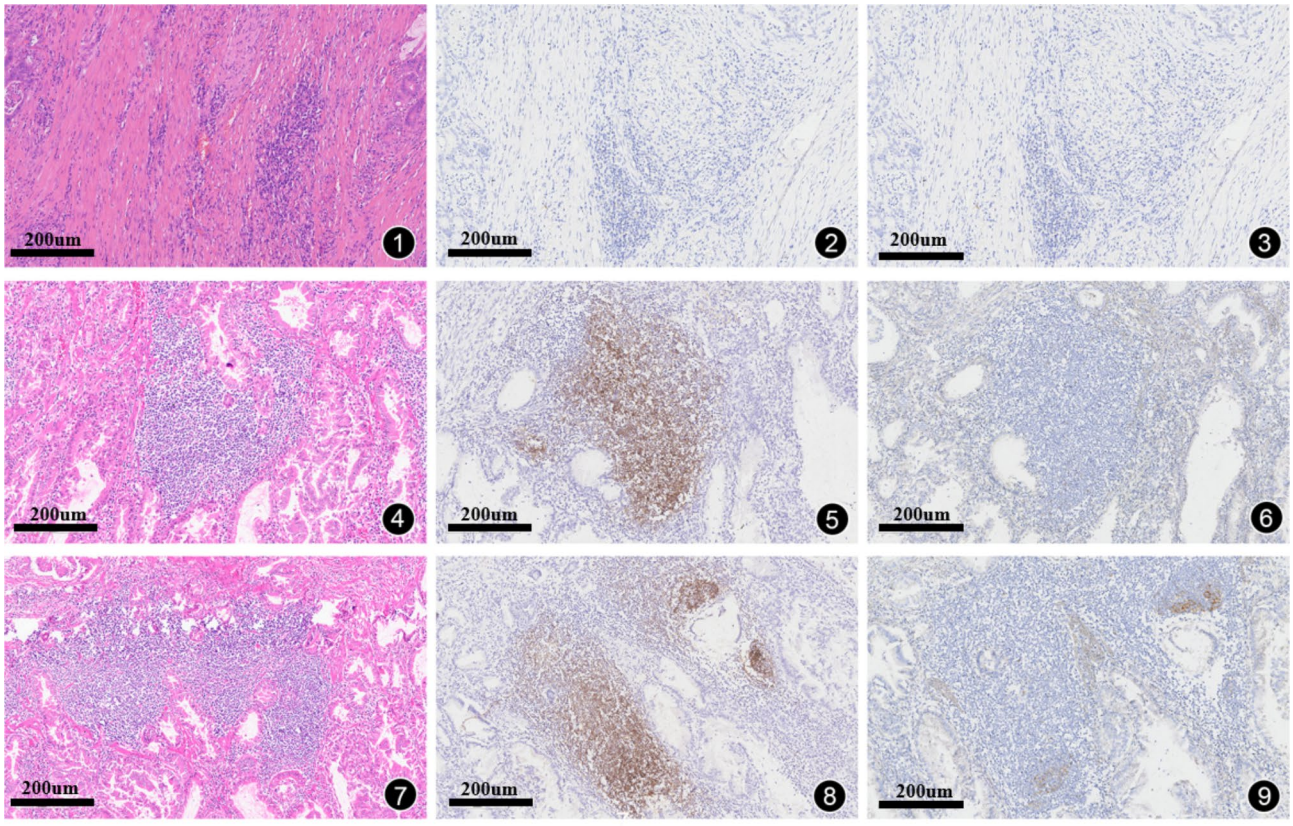

Fig. 5 Heterogeneity of IT-TLS maturity. (1) E-TLS, HE staining; (2) CD21-negative in E-TLS, EnVision method; (3) CD23-negative in E-TLS, EnVision method; (4) PEL-TLS, HE staining; (5) CD21-positive in PEL-TLS, EnVision method; (6) CD23-negative in PEL-TLS, EnVision method; (7) SFL-TLS, HE staining; (8) CD21-positive in SFL-TLS, EnVision method; (9) CD23-positive in SFL-TLS, EnVision method. The scale bars on the H&E and immunohistochemical images indicate 200 μm

[20]. Additionally, our analysis revealed that PT-TLS were more numerous and had a longer maximum diameter compared to both IT-TLS and IM-TLS. This observation may be attributed to the unique immunological characteristics of the intestine, which is considered the largest immune organ in the human body. The small intestinal mucosa is particularly rich in lymphocytes, facilitating the development and maintenance of TLS. This may also be related to the reported presence of γδT cells in the small intestinal mucosal aggregates, although the underlying biological mechanisms require further exploration [21]. We also observed that TLS existed in different spatial locations, which is consistent with the findings reported in colorectal cancer [20].

Furthermore, this study used immunohistochemical staining results and digital pathology image analysis software to further determine the maturity and density of TLS. Regarding the location of TLS in tumors, the presence of PT-TLS has been reported in most tumors, while some tumors also have IT-TLS, such as renal clear cell carcinoma lung metastasis, hepatocellular carcinoma, and germ cell tumors [22–24]. However, previous studies have only generally differentiated between IT-TLS and PT-TLS, without specifically distinguishing whether the PT-TLS are located at the invasive margin or in the stroma or normal tissue distant from the tumor [25]. Therefore, in this study, with the assistance of digital pathology image analysis software, the intratumoral location of TLS was standardized, and we hypothesized that TLS in three different locations - IT, IM, and PT - may have certain prognostic implications. TLS were quantitatively and spatially analyzed. Based on this, we categorized TLS into three spatial locations (IT, IM, PT) and three maturity stages (E-TLS, PEL-TLS, SFL-TLS).

Interestingly, we observed that the invasive margin was mainly composed of SFL-TLS, while IT-TLS were predominantly E-TLS. This finding is in contrast to Xu et al.'s study in renal clear cell carcinoma [26], where proximal TLS were mainly SFL-TLS, while distal TLS were primarily E-TLS. Theoretically, as Ding described [27], IT-TLS, being closer to the tumor cells, may have a stronger antitumor immune response compared to PT-TLS. However, in our study cohort, IT-TLS had a lower density and were mostly early-stage TLS. In contrast, the density of IM-TLS was significantly higher than that of IT-TLS, with SFL-TLS being the main component. We speculate that

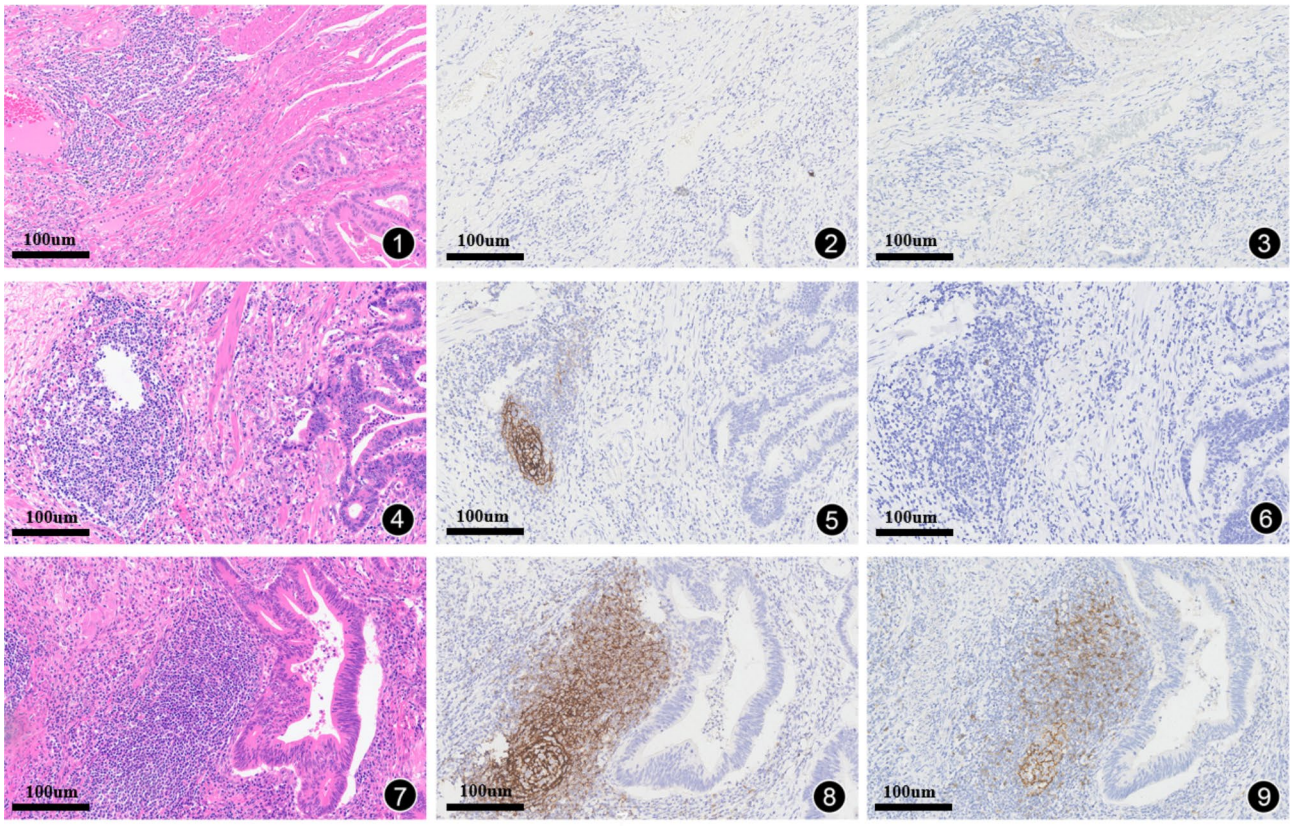

Fig. 6 Heterogeneity of IM-TLS maturity. (1) E-TLS, HE staining; (2) CD21-negative in E-TLS, EnVision method; (3) CD23-negative in E-TLS, EnVision method; (4) PEL-TLS, HE staining; (5) CD21-positive in PEL-TLS, EnVision method; (6) CD23-negative in PEL-TLS, EnVision method; (7) SFL-TLS, HE staining; (8) CD21-positive in SFL-TLS, EnVision method; (9) CD23-positive in SFL-TLS, EnVision method. The scale bars on the H&E and immunohistochemical images indicate 100 μm

this may be partially related to the relatively smaller spatial area of the invasive margin region, but there are differences in the maturity of TLS in different locations, and the driving factors and mechanisms behind this require further exploration.

It is well known that TLS are associated with better clinical prognosis in various tumors, such as pancreatic neuroendocrine tumors, lung cancer, and breast cancer [28–30]. However, there have also been reports of differences between primary and metastatic lesions in different tumors. Cipponi et al. [31] found in a study of malignant melanoma that TLS were not observed in primary lesions but were present in metastatic lesions. Lee et al. [32] included 335 cases of metastatic breast cancer from four different metastatic sites and found that almost all metastatic lesions had TILs, but only liver and lung metastases had TLS. Taken together, these data suggest that the predictive role of TLS in prognosis may be influenced by the overall quantity, activity, composition of cell components, and surrounding microenvironment of TLS. In our study, based on the maturity of TLS, we only observed a favorable effect of high-density SFL-TLS and E-TLS on reducing the risk of tumor metastasis/recurrence, but there was no statistically significant difference in extending OS. In terms of spatial location, high-density PT-TLS showed a trend towards prolonged OS.

To further assess the role of TLS in tumor progression, we analyzed the relationship between TLS density and clinical pathological features. We found that high-density TLS was more likely detected in patients with lower T stages, no mucinous components, no tumor nodules, and no distant metastases. This indirectly suggests that high-density TLS may have predictive value for a favorable prognosis in this type of tumor to some extent. This aligns with previous findings showing that tumors in the high-density TLS group tend to be smaller, particularly in liver cancer, gastric cancer, and colorectal cancer [33, 34]. Thus, researchers have proposed that TLS density might play a role in controlling growth in colorectal cancer [34]. The intestinal tract contains abundant lymphatic vessels and blood vessels, and this specialized vascular system may play a potential guiding and transport role in the recruitment of follicular dendritic cells and lymphocytes [35, 36]. Therefore, studying the prognostic significance of TLS in primary adenocarcinoma of jejunum and ileum patients is valuable. Given that this tumor is rare, more

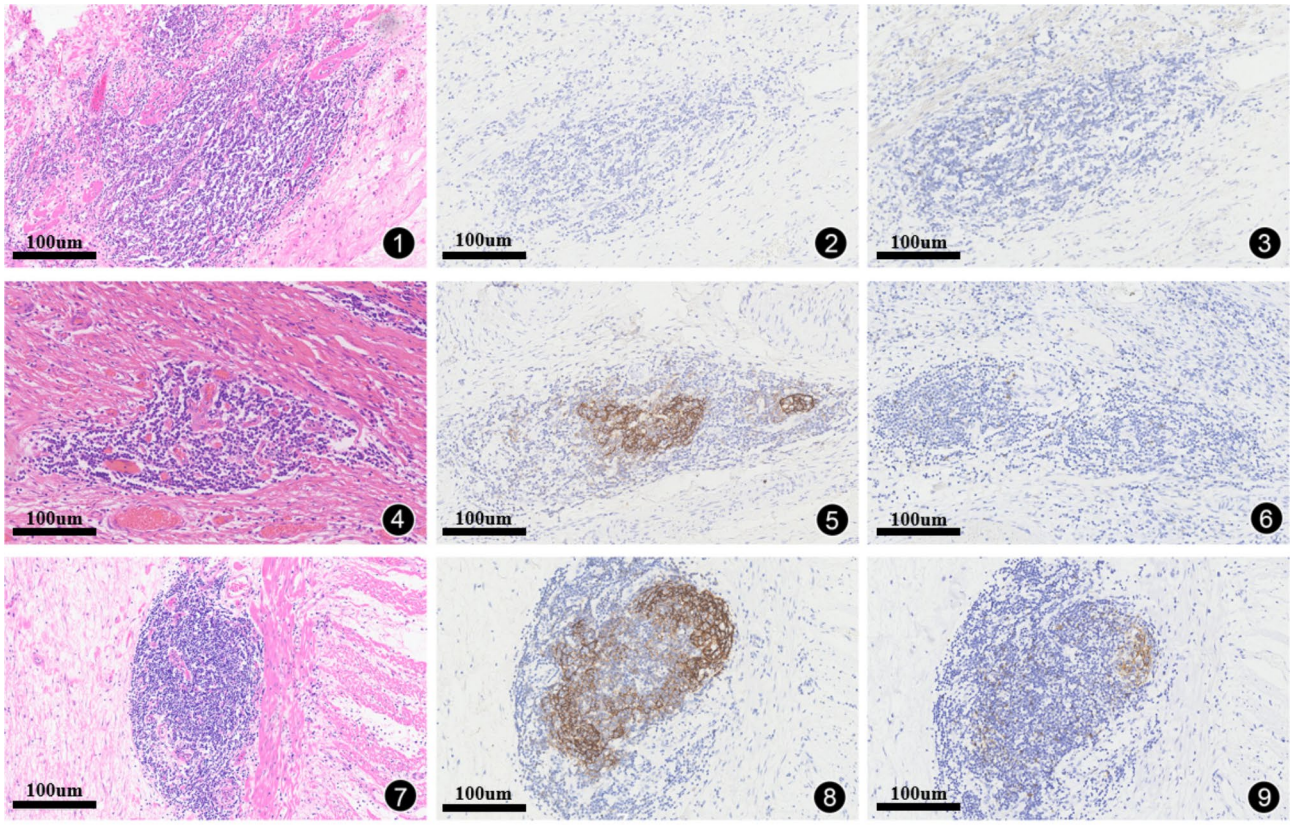

Fig. 7 Heterogeneity of PT-TLS maturity. (1) E-TLS, HE staining; (2) CD21-negative in E-TLS, EnVision method; (3) CD23-negative in E-TLS, EnVision method; (4) PEL-TLS, HE staining; (5) CD21-positive in PEL-TLS, EnVision method; (6) CD23-negative in PEL-TLS, EnVision method; (7) SFL-TLS, HE staining; (8) CD21-positive in SFL-TLS, EnVision method; (9) CD23-positive in SFL-TLS, EnVision method. The scale bars on the H&E and immunohistochemical images indicate 100 μm

cases will need to be collected in the future for further validation.

Immunotherapy has improved the natural course and clinical prognosis of many solid tumors. Immune markers such as MSI, TMB, and high expression of PD-L1 in tumor cells play an important role in predicting the response of patients to immune checkpoint inhibitors and other immunotherapeutic drugs. A study involving 106 cases of small bowel adenocarcinoma (SBA) showed that approximately 14.2% exhibited MSI-H/dMMR [37]. Schrock et al. conducted a large-scale study exploring the genomic phenotypes of SBA and other gastrointestinal tumors and found that 7.6% (13/170) of SBA cases showed MSI-H, compared to 4% and 3.9% in colorectal cancer and gastric cancer, respectively [38]. In our study, only 6 cases (11.1%) were found to be MSI-H, which is consistent with the literature. It has been reported that approximately 9.5% of SBA cases have a high mutational burden (>20 mut/Mb), while the incidence in colorectal cancer and gastric cancer is 4.3% and 5.6%, respectively. Interestingly, among the 13 MSI-H tumors in SBA, approximately 92.3-100% had a high TMB. Additionally, compared to duodenal adenocarcinoma, the TMB of SBA without specific site designation was significantly higher ($P=0.046$) [38]. In our study cohort, 42.6% (23/54) showed TMB-H, and the incidence of TMB-H was 24.2% (8/33) in the TLS+group. TMB-H tumors were more likely to occur in the ileum, which is slightly higher than the reported proportion, and we speculate that this may be because the duodenal cases were not included in this study and TMB-H is more common in primary adenocarcinoma of jejunum and ileum, consistent with the aforementioned literature. Furthermore, there was a significant positive correlation between TMB-H and MSI-H in our study cohort, which was also confirmed in the TLS+group, providing data support for future immunotherapy in primary adenocarcinoma of jejunum and ileum to some extent.

Pedersen et al. [39] conducted PD-L1 immunohistochemical testing on 45 SBA patients, and the results showed that 53.3% (24/45) of tumors exhibited positive expression of PD-L1. Survival analysis revealed a significant association between positive expression of PD-L1 in tumor cells and shorter median OS. In a large study involving 121 SBA cases, immunohistochemical staining for PD-L1 showed that the proportion of patients

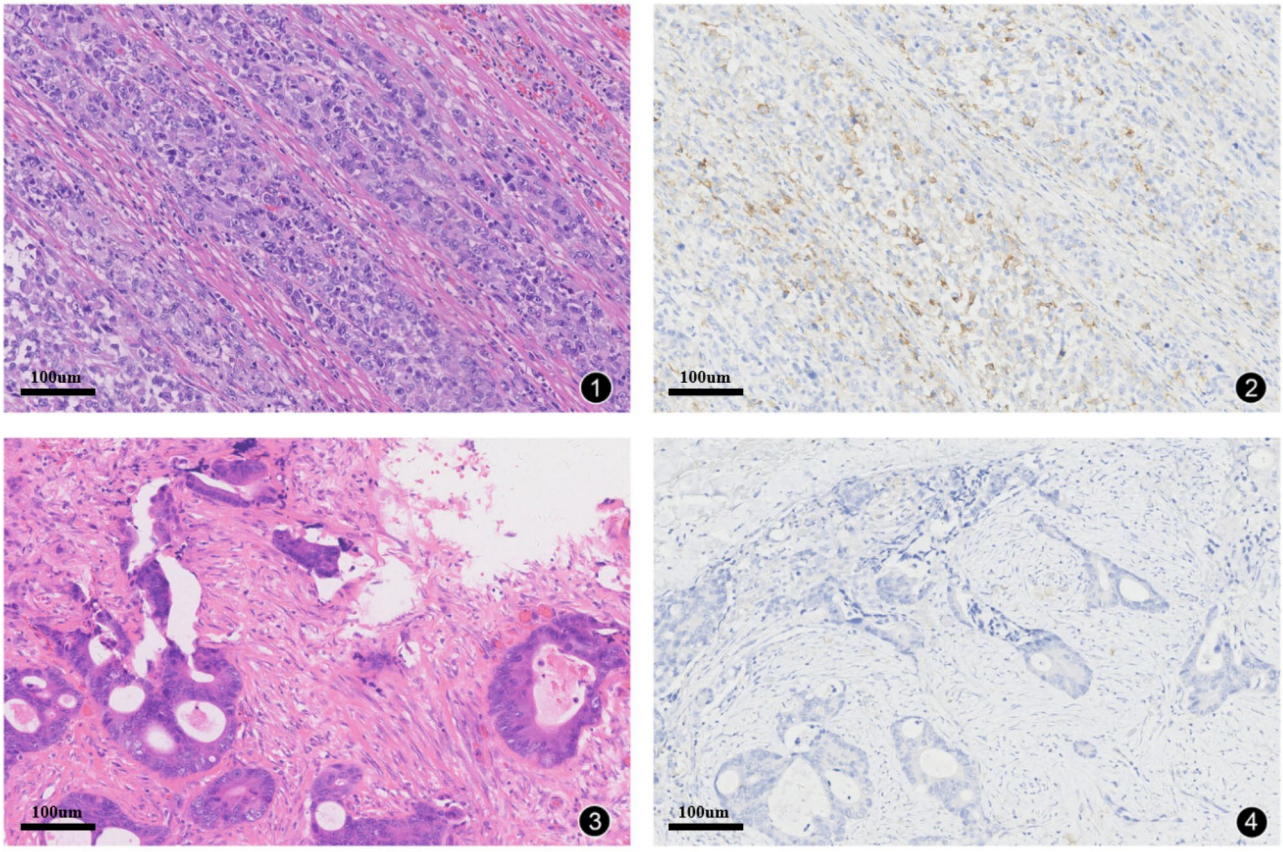

Fig. 8 Expression of PD-L1 (22C3) in primary adenocarcinoma of jejunum and ileum. (1) This case shows poorly differentiated adenocarcinoma with diffuse distribution and loss of adhesion, H&E staining. (2) PD-L1 (22C3) CPS > 1, EnVision method. (3) This case shows moderately differentiated adenocarcinoma, H&E staining. (4) PD-L1 (22C3) CPS < 1, EnVision method. The scale bars on the H&E and immunohistochemical images indicate 100 μm

with CPS≥1 was 26%. Furthermore, in MSI-H cases, the incidence of CPS≥1 SBA was significantly higher than in non-MSI-H cases [40]. In our study cohort, CPS≥1 cases accounted for 33.33% (18/54) of the entire primary adenocarcinoma of jejunum and ileum cohort and 33.33% (11/33) of the TLS+group. However, the incidence of CPS≥1 group in MSI-H cases was not significantly higher than in non-MSI-H cases (50% vs. 31.25%, $P=0.844$). This may be related to the small number of cases and requires further data accumulation for interpretation. Numerous clinical trials have demonstrated the efficacy of anti-PD-1 and anti-CTLA4 checkpoint inhibitors in MSI-H subtype tumors and tumors with high TMB [41, 42]. In a large phase II clinical trial involving 40 previously treated advanced SBA patients, pembrolizumab was prospectively evaluated for its efficacy in advanced SBA and partial responses were observed in two TMB-H patients [43]. In our study cohort, TMB-H tumors also exhibited higher levels of PD-L1 expression and were more likely to occur in patients without distant metastasis, with lower TNM stages, negative lymphovascular invasion, and higher TLS density, suggesting that TMB-H may potentially predict the response to immune checkpoint therapy to some extent. Additionally, Jun et al. [44] found in the genetic data of 190 SBA patients that patients with *KRAS* or *BRAF* gene mutations had shorter survival than those with wild-type *KRAS*. *KRAS* oncogene mutation was an independent predictor of poor prognosis in SBA with lower T stages. However, in our study cohort, we observed that the probability of *KRAS* gene mutation was lower in tumors classified as TMB-H. Additionally, the incidence of *NRAS* gene mutation was reduced in TLS+group. These findings suggest that both TMB-H status and the presence of TLS may carry predictive significance for targeted therapies, such as anti-EGFR therapy, in primary adenocarcinoma of jejunum and ileum.

Currently, this study has several limitations, primarily due to the retrospective nature of the enrolled cases. Retrospective studies inherently come with constraints that could impact the clinical significance of the findings. To address these limitations, future research should focus on designing well-structured prospective clinical trials. Such trials would help validate the findings, identify more sensitive and reliable biomarkers, and enhance the clinical applicability of the results for immunotherapy and

Table 2 Relationship among TLS, PD-L1(22C3), TMB and clinical pathological features in 54 patients with primary adenocarcinoma of jejunum and ileum

Clinical pathological features		Cases	TLS		χ2	*P* value	PD-L1(22C3)		χ2	*P* value	TMB		χ2	*P* value
			Yes	No			CPS ≥ 1	CPS<1			High	Low		
Age(y)	≤ 60	29	20	9	1.626	0.202	10	19	0.037	0.847	10	19	1.685	0.194
	>60	25	13	12			8	17			13	12		
Sex	M	30	10	11	0.140	1.708	9	21	0.338	0.561	15	15	1.515	0.218
	F	24	14	10			9	15			8	16		
Tumor site	Jejunum	38	27	11	5.334	0.021	13	25	0.044	0.833	12	26	6.362	0.012
	Ileum	16	6	10			5	11			11	5		
Tumor size(cm)	≤ 5	38	23	15	0.018	0.892	11	27	1.110	0.292	14	24	1.734	0.188
	>5	16	10	8			7	9			9	7		
Macroscopic tumor perforation	Yes	3	2	1	0.041	0.839	2	1	1.588	0.208	2	1	0.753	0.386
	No	51	31	20			16	35			21	30		
Differentiation grade	Moderately differentiation	34	22	12	0.567	0.451	8	26	6.110	0.013	12	22	1.402	0.236
	Poorly differentiation	15	8	7			9	6			8	7		
Lymphatic invasion	Yes	27	21	6	6.317	0.012	9	18	0.000	1.000	9	18	1.893	0.169
	No	27	12	15			9	18			14	13		
Vascular invasion	Yes	19	10	9	0.887	0.346	7	12	0.162	0.687	9	10	0.273	0.601
	No	35	23	12			11	24			14	21		
Neural invasion	Yes	36	22	14	0.000	1.000	8	28	6.000	0.014	14	22	0.606	0.436
	No	18	11	7			10	8			9	9		
Tumor nodules	Yes	15	11	4	1.305	0.253	6	9	0.415	0.519	6	9	0.057	0.811
	No	39	22	17			12	27			17	22		
Mucinous component	Yes	12	7	5	0.050	0.823	1	11	4.339	0.037	5	7	0.005	0.941
	No	42	26	16			17	25			18	24		
T stage	T3	18	12	6	0.351	0.554	7	11	0.375	0.540	7	11	0.151	0.697
	T4	36	21	15			11	25			16	20		
N stage	N0	40	22	18	2.424	0.119	12	28	0.771	0.380	17	23	0.001	0.981
	N1-3	14	11	3			6	8			6	8		
M stage	M0	30	16	14	1.718	0.190	14	16	5.400	0.020	17	13	5.468	0.019
	M1	24	17	7			4	20			6	18		
TNM stage	II	24	12	12	2.279	0.320	9	15	9.938	0.007	12	12	7.649	0.022
	III	6	4	2			5	1			5	1		
	IV	24	17	7			4	20			6	18		
PD-L1(22C3)	CPS ≥ 1	18	11	7	0.000	1.000					11	7	3.787	0.052
	CPS<1	36	22	14							12	24		
MSI-H	Yes	6	3	3	0.351	0.554	3	3	0.844	0.358	6	0	9.098	0.003
	No	48	30	18			15	33			17	31		
TMB	High	23	12	11	1.347	0.246								
	Low	31	21	10										

Table 2 (continued)

Clinical pathological features		Cases	TLS		χ2	*P* value	PD-L1(22C3)		χ2	*P* value	TMB		χ2	*P* value
			Yes	No			CPS ≥ 1	CPS<1			High	Low		
KRAS mutation	Yes	30	17	13	0.561	0.454	10	20	0.000	1.000	9	21	4.378	0.036
	No	24	16	8			8	16			14	10		
NRAS mutation	Yes	2	0	2	3.264	0.071	0	2	1.038	0.308	1	1	0.047	0.829
	No	52	33	19			18	34			22	30		
BRAF mutation	Yes	3	2	1	0.041	0.839	2	1	1.588	0.208	1	2	0.111	0.739
	No	51	31	20			16	35			22	29		
PIK3CA mutation	Yes	4	1	3	2.370	0.124	2	2	0.540	0.462	3	1	1.856	0.173
	No	50	32	18			16	34				30		

targeted therapy. Second, the rarity of this tumor type poses significant challenges in collecting sufficient fresh tumor tissues for analysis. As a result, we relied on immunohistochemistry and next-generation sequencing using FFPE samples to evaluate the maturity of TLS and associated immune predictive markers. While these methods provide valuable insights, they may not offer the same level of accuracy and detail as more advanced techniques, such as flow cytometry or spatial transcriptomics. Future studies that can access fresh tumor samples would benefit from employing these more sophisticated methodologies, potentially leading to a deeper understanding of the immune landscape and further elucidating the prognostic significance of TLS in primary adenocarcinoma of jejunum and ileum. Third, we only roughly assessed the cellular composition and proportions of TLS, and whether there are other factors that can induce or interfere with the anti-tumor immune effects of TLS remains to be explored. It is worth investigating further. In the future, we hope to utilize advanced techniques such as single-cell sequencing or spatial transcriptomics to delve deeper into the microscopic changes of TLS. This will allow for a more comprehensive understanding of the functional mechanisms of TLS in the tumor microenvironment. Finally, this cohort is only a single-center study, and although efforts were made to collect and organize the data, the sample size is still insufficient. Furthermore, the specific role and mechanisms of spatial localization and maturity heterogeneity of TLS in the tumor microenvironment of primary adenocarcinoma of jejunum and ileum were not further explored. It is expected that future studies will accumulate more samples and clinical data from multiple centers and explore the changes in the tumor microenvironment of primary adenocarcinoma of jejunum and ileum at the cellular and animal experimental levels.

In conclusion, this study provides the first insights into the impact of spatial localization and maturity heterogeneity of TLS on the progression and immune response in primary adenocarcinoma of jejunum and ileum. By combining digital pathology image analysis software and next-generation sequencing technology, the association between TMB, immune checkpoint molecules (such as PD-L1), MSI, and TLS was investigated in a more accurate manner. Most TLS were located at the invasive margin and peritumoral region, with mature TLS being predominant at the invasive margin and immature TLS being predominant intratumorally. It is worth noting that TMB was closely associated with MSI and PD-L1, suggesting its potential predictive value for immunotherapy in primary adenocarcinoma of jejunum and ileum.

Table 3 Relationship among PD-L1(22C3), TMB and clinical pathological features in 33 patients with TLS + primary adenocarcinoma of jejunum and ileum

Clinical pathological features		Cases	TMB		*P* value	PD-L1(22C3)		*P* value
			High	Low		CPS ≥ 1	CPS<1	
Age(y)	≤ 60	20	3	13	1	7	13	1
	>60	13	5	8		4	9	
Sex	M	19	8	11	0.486	6	13	1
	F	14	4	10		5	9	
Tumor site	Jejunum	27	8	19	0.159	10	17	0.637
	Ileum	6	4	2		1	5	
Tumor size(cm)	≤ 5	23	7	16	0.433	5	18	0.049
	>5	10	5	5		6	4	
Macroscopic tumor perforation	Yes	2	1	1	1	1	1	1
	No	31	11	10		10	21	
Differentiation grade	Moderately differentiation	22	8	14	1	5	17	0.078
	Poorly differentiation	8	3	5		5	3	
Lymphatic invasion	Yes	21	5	16	0.067	6	15	1
	No	12	7	5		5	7	
Vascular invasion	Yes	10	5	5	0.433	3	7	1
	No	23	7	16		8	15	
Neural invasion	Yes	22	7	15	0.471	4	18	0.017
	No	11	5	6		7	4	
Tumor nodules	Yes	11	4	7	1	5	6	0.437
	No	22	8	14		6	16	
Mucinous component	Yes	7	3	4	0.686	1	6	0.378
	No	26	9	17		10	16	
T stage	T3	12	4	8	1.000	5	7	0.471
	T4	21	8	13		6	15	
N stage	N0	22	8	13	1.000	7	15	1.000
	N1-3	11	4	7		4	7	
M stage	M0	16	8	8	0.157	7	9	0.282
	M1	17	4	13		4	13	
TNM stage	II	12	5	7	0.716	4	8	1
	III-IV	21	7	14		7	14	
PD-L1(22C3)	CPS ≥ 1	11	5	6	0.471			
	CPS<1	22	7	15				
MSI-H	Yes	3	3	0	0.04	1	2	1
	No	30	9	21		10	20	
KRAS mutation	Yes	17	4	13	0.157	5	12	0.721
	No	16	8	8		6	10	
BRAF mutation	Yes	31	11	20	1	10	21	1
	No	2	1	1		1	1	
PIK3CA mutation	Yes	1	1	0	0.364	1	0	1
	No	32	11	21		11	21	

Table 4 Kaplan-Meier survival analysis of clinicopathological parameters of 33 patients with TLS + primary adenocarcinoma of jejunum and ileum

Variables		Single factor (OS)		Single factor (DFS)	
		95% confidence interval	*P* value	95% confidence interval	*P* value
Age(y)	≤ 60	38.69-77.383	0.698	9.082–32.323	0.323
	>60	43.115–78.828		12.586–46.852	
Sex	M	61.438–86.828	0.056	13.949–42.978	0.281
	F	22.991–57.439		6.4-31.171	
Tumor site	Jejunum	48.807–81.099	0.816	17.319–42.457	0.292
	Ileum	34.287–77.313		5.071–25.679	
Tumor size(cm)	≤ 5	39.025–67.791	0.559	14.822–38.831	0.382
	>5	39.493–95.507		6.007–16.513	
Macroscopic tumor perforation	Yes	/	0.641	16–16	0.976
	No	/		14.292–35.323	
Differentiation grade	Moderately differentiation	49.663–83.055	0.069	14.66-41.786	0.315
	Poorly differentiation	15.346–50.154		2.11–35.89	
Lymphatic invasion	Yes	29.904–55.68	0.123	9.786–29.288	0.249
	No	61.533–90.689		10.265–49.548	
Vascular invasion	Yes	45.457–94.543	0.576	5.149–12.751	0.121
	No	38.917–67.534		15.544–39.135	
Neural invasion	Yes	37.327–56.563	0.365	13.546–32.135	0.814
	No	47.659–93.941		0-42.441	
Tumor nodules	Yes	16.303–24.437	0.046	0-36.926	0.611
	No	51.44-82.607		14.003–32.73	
Mucinous component	Yes	21.398–42.019	0.417	2.219–32.225	0.779
	No	47.682–79.649		13.15-35.543	
T stage	T3	42.434–86.709	0.822	14.968–47.342	0.628
	T4	40.058–70.742		9.685–27.53	
N stage	N0	60.597–89.403	< 0.001	10.851–40.598	< 0.001
	N1-3	14.458–40.66		9.208–34.637	
M stage	M0	/	0.044	28.455–66.045	0.001
	M1	/		4.8-19.409	
TNM stage	II	/	0.077	21.756–66.703	0.011
	III-IV	/		7.385–23.373	
TLS density	High	42.826–79.386	0.414	12.885–43.104	0.293
	Low	36.453–75.365		7.15-27.728	
IT-TLS density	High	39.958–60.476	0.924	13.62-39.483	0.382
	Low	42.371–82.977		8.137–32.025	
IM-TLS density	High	37.14-60.638	0.859	12.822–40.784	0.416
	Low	41.233–82.989		7.753–30.584	
PT-TLS density	High	46.521–84.933	0.090	10.385–20.393	0.941
	Low	21.564–65.486		10.376–38.663	
E-TLS	High	41.732–55.601	0.383	18.005–54.545	0.069
	Low	38.619–74.989		7.438–24.209	
PEL-TLS	High	41.562–56.438	0.293	16.443–41.343	0.356
	Low	35.253–72.567		9.046–31.943	
SFL-TLS	High	36.388–76.541	0.966	17.983–54.817	0.047
	Low	47.054–76.032		6.958–23.413	
PD-L1(22C3)	CPS ≥ 1	54.648–92.495	0.565	4.34-15.041	0.265
	CPS<1	37.597–66.87		14.75-38.203	
MSI-H	Yes	/	0.450	13.066–21.601	0.486
	No	/		12.819–33.635	
TMB	H	51.79–89.21	0.128	9.974–21.749	0.962
	L	33.167–67.775		13.399–38.305	

Table 4 (continued)

Variables		Single factor (OS)		Single factor (DFS)	
		95% confidence interval	*P* value	95% confidence interval	*P* value
KRAS gene	Mutation	28.885–52.582	0.579	7.154–15.414	0.579
	Wild	42.42-80.398		14.91-41.938	
BRAF gene	Mutation	/	/	/	0.457
	Wild	/		/	
PIK3CA gene	Mutation	57–57	0.644	23–23	0.939
	Wild	50.446–79.535		14.737–36.027	

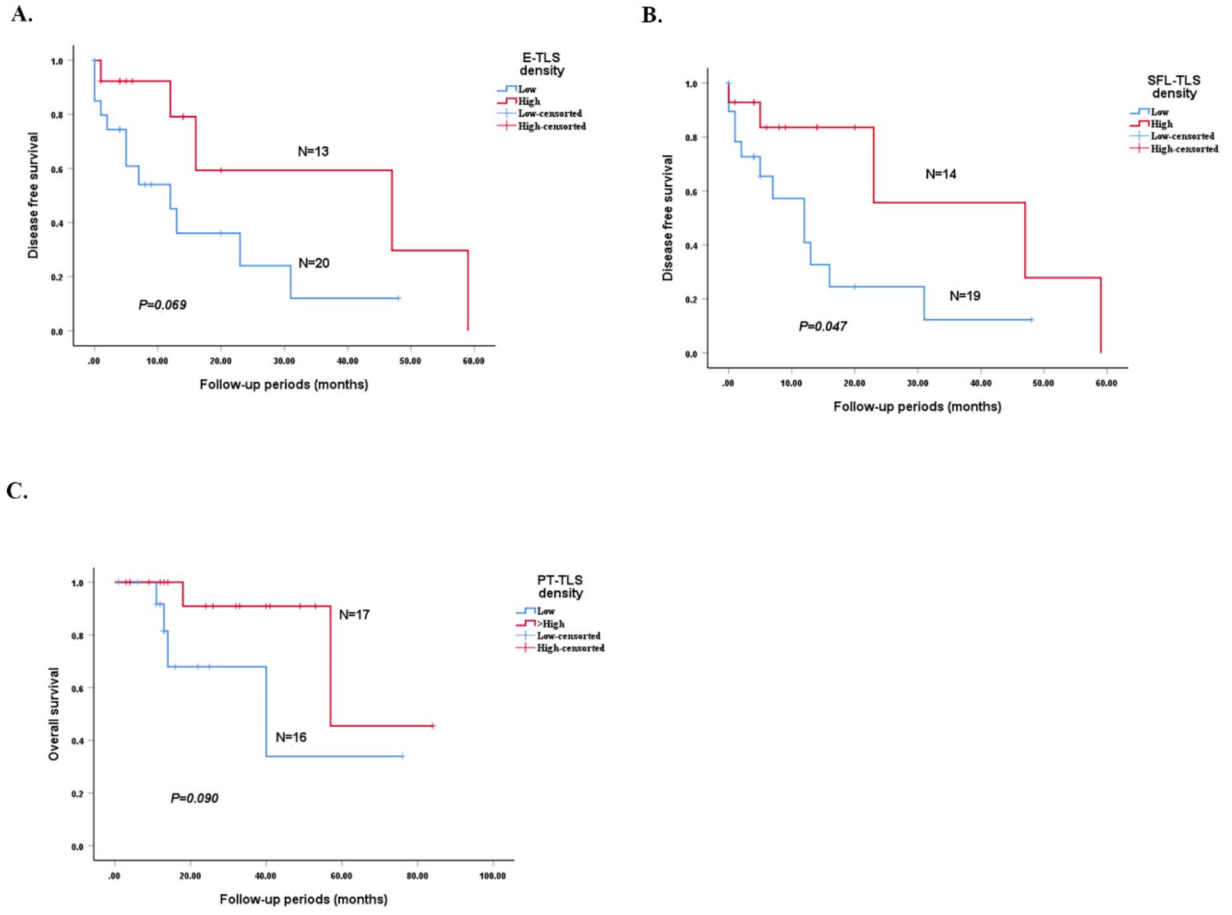

Fig. 9 The impact of spatial positioning and maturity of TLS on DFS and OS in primary adenocarcinoma of jejunum and ileum patients. (**A**) In terms of TLS maturity, the E-TLS-high group showed a trend of prolonged DFS compared to the E-TLS-low group ($P=0.069$); (**B**) In terms of TLS maturity, the SFL-TLS-high group had a longer DFS time compared to the SFL-TLS-low group ($P=0.047$); (**C**) In terms of TLS spatial positioning, the PT-TLS-high group showed a trend of prolonged OS compared to the PT-TLS-low group ($P=0.090$)

Author contributions
Conceptualization, M.Y.D; Methodology, Y.J; Software, X.L; Data Curation, M.Y.D and R.K.L; Investigation, X.L and Y.J; Resources, L.X, X.L.Z and J.A.K.S.S; Writing – Original Draft Preparation, M.Y.D; Writing – Review & Editing, Y.Y.H; Visualization, M.Y.D; Supervision, C.X; Funding Acquisition, Y.Y.H. All authors contributed to data interpretation, manuscript editing, and revision.

Funding
The study was supported by the National Clinical Key Specialty Project - Next-generation Integrated Pathological Diagnosis of Oncologic Diseases under the Department of Pathology (YWP2023-001); Shanghai Clinical Specialty Construction Project (shslczdzk01302); Shanghai Science and Technology Innovation Action Plan - Natural Science Foundation Project (23ZR1410000); Shanghai Science and Technology Innovation Action Plan - Natural Science Foundation Project (23ZR1410200).

Data availability
No datasets were generated or analysed during the current study.

Declarations

Ethics approval and consent to participate
The participant in our study provided signed informed consent. This study was approved by the ethics committee of the Zhongshan Hospital, Fudan University, and the IRB is B2023-304R.

Consent for publication
Not applicable.

Competing interests
The authors declare no competing interests.

Received: 3 July 2024 / Accepted: 21 September 2024
Published online: 30 September 2024

References

1. Bhamidipati D, Colina A, Hwang H, et al. Metastatic small bowel adenocarcinoma: role of metastasectomy and systemic chemotherapy. ESMO Open. 2021;6(3):100132.
2. Guan WL, He Y, Xu RH. Gastric cancer treatment: recent progress and future perspectives. J Hematol Oncol. 2023;16(1):57.
3. Debien V, De Caluwé A, Wang X, et al. Immunotherapy in breast cancer: an overview of current strategies and perspectives. NPJ Breast Cancer. 2023;9(1):7.
4. Sun X, Liu W, Sun L, et al. Maturation and abundance of tertiary lymphoid structures are associated with the efficacy of neoadjuvant chemoimmunotherapy in resectable non-small cell lung cancer. J Immunother Cancer. 2022;10(11):e005531.
5. Maibach F, Sadozai H, Seyed Jafari SM, Hunger RE, Schenk M. Tumor-infiltrating lymphocytes and their prognostic value in cutaneous melanoma. Front Immunol. 2020;11:2105.
6. Hiraoka N, Ino Y, Yamazaki-Itoh R, Kanai Y, Kosuge T, Shimada K. Intratumoral tertiary lymphoid organ is a favourable prognosticator in patients with pancreatic cancer. Br J Cancer. 2015;112(11):1782–90.
7. Nakamura S, Ohuchida K, Hayashi M, et al. Tertiary lymphoid structures correlate with enhancement of antitumor immunity in esophageal squamous cell carcinoma. Br J Cancer. 2023;129(8):1314–26.
8. Vaddepally RK, Kharel P, Pandey R, Garje R, Chandra AB. Review of indications of FDA-Approved Immune Checkpoint inhibitors per NCCN guidelines with the level of evidence. Cancers (Basel). 2020;12(3):738.
9. Davis AA, Patel VG. The role of PD-L1 expression as a predictive biomarker: an analysis of all US Food and Drug Administration (FDA) approvals of immune checkpoint inhibitors. J Immunother Cancer. 2019;7(1):278.
10. Schumacher TN, Thommen DS. Tertiary lymphoid structures in cancer. Science. 2022;375(6576):eabf9419.
11. Karjula T, Niskakangas A, Mustonen O, et al. Tertiary lymphoid structures in pulmonary metastases of microsatellite stable colorectal cancer. Virchows Arch. 2023;483(1):21–32.
12. Zhang C, Wang XY, Zuo JL, et al. Localization and density of tertiary lymphoid structures associate with molecular subtype and clinical outcome in colorectal cancer liver metastases. J Immunother Cancer. 2023;11(2):e006425.
13. Hendry S, Salgado R, Gevaert T, et al. Assessing tumor-infiltrating lymphocytes in solid tumors: a practical review for pathologists and proposal for a standardized method from the International Immuno-Oncology biomarkers Working Group: part 2: TILs in Melanoma, gastrointestinal Tract Carcinomas, Non-small Cell Lung Carcinoma and Mesothelioma, endometrial and ovarian carcinomas, squamous cell carcinoma of the Head and Neck, Genitourinary Carcinomas, and primary brain tumors. Adv Anat Pathol. 2017;24(6):311–35.
14. Siliņa K, Soltermann A, Attar FM, et al. Germinal centers determine the prognostic relevance of Tertiary lymphoid structures and are impaired by corticosteroids in Lung squamous cell carcinoma. Cancer Res. 2018;78(5):1308–20.
15. Helmink BA, Reddy SM, Gao J, et al. B cells and tertiary lymphoid structures promote immunotherapy response. Nature. 2020;577(7791):549–55.
16. van Dijk N, Gil-Jimenez A, Silina K, et al. Preoperative ipilimumab plus nivolumab in locoregionally advanced urothelial cancer: the NABUCCO trial. Nat Med. 2020;26(12):1839–44.
17. Cabrita R, Lauss M, Sanna A, et al. Author correction: tertiary lymphoid structures improve immunotherapy and survival in melanoma. Nature. 2020;580(7801):E1.
18. Darvin P, Toor SM, Sasidharan Nair V, Elkord E. Immune checkpoint inhibitors: recent progress and potential biomarkers. Exp Mol Med. 2018;50(12):1–11.
19. Kulangara K, Zhang N, Corigliano E, et al. Clinical utility of the combined positive score for programmed death Ligand-1 expression and the approval of Pembrolizumab for treatment of gastric Cancer. Arch Pathol Lab Med. 2019;143(3):330–7.
20. Wang Q, Shen X, An R, et al. Peritumoral tertiary lymphoid structure and tumor stroma percentage predict the prognosis of patients with non-metastatic colorectal cancer. Front Immunol. 2022;13:962056.
21. Sullivan ZA, Khoury-Hanold W, Lim J, et al. γδ T cells regulate the intestinal response to nutrient sensing. Science. 2021;371(6535):eaba8310.
22. Willis SN, Mallozzi SS, Rodig SJ, et al. The microenvironment of germ cell tumors harbors a prominent antigen-driven humoral response. J Immunol. 2009;182(5):3310–7.
23. Calderaro J, Petitprez F, Becht E, et al. Intra-tumoral tertiary lymphoid structures are associated with a low risk of early recurrence of hepatocellular carcinoma. J Hepatol. 2019;70(1):58–65.
24. Remark R, Alifano M, Cremer I, et al. Characteristics and clinical impacts of the immune environments in colorectal and renal cell carcinoma lung metastases: influence of tumor origin. Clin Cancer Res. 2013;19(15):4079–91.
25. Munoz-Erazo L, Rhodes JL, Marion VC, Kemp RA. Tertiary lymphoid structures in cancer - considerations for patient prognosis. Cell Mol Immunol. 2020;17(6):570–5.
26. Xu W, Lu J, Liu WR, et al. Heterogeneity in tertiary lymphoid structures predicts distinct prognosis and immune microenvironment characterizations of clear cell renal cell carcinoma. J Immunother Cancer. 2023;11(12):e006667.
27. Ding GY, Ma JQ, Yun JP, et al. Distribution and density of tertiary lymphoid structures predict clinical outcome in intrahepatic cholangiocarcinoma. J Hepatol. 2022;76(3):608–18.
28. Zhang WH, Wang WQ, Han X, et al. Infiltrating pattern and prognostic value of tertiary lymphoid structures in resected non-functional pancreatic neuroendocrine tumors. J Immunother Cancer. 2020;8(2):e001188.
29. Goc J, Fridman WH, Hammond SA, Sautès-Fridman C, Dieu-Nosjean MC. Tertiary lymphoid structures in human lung cancers, a new driver of antitumor immune responses. Oncoimmunology. 2014;3:e28976.
30. Posch F, Silina K, Leibl S, et al. Maturation of tertiary lymphoid structures and recurrence of stage II and III colorectal cancer. Oncoimmunology. 2017;7(2):e1378844.
31. Cipponi A, Mercier M, Seremet T, et al. Neogenesis of lymphoid structures and antibody responses occur in human melanoma metastases. Cancer Res. 2012;72(16):3997–4007.
32. Lee M, Heo SH, Song IH, et al. Presence of tertiary lymphoid structures determines the level of tumor-infiltrating lymphocytes in primary breast cancer and metastasis. Mod Pathol. 2019;32(1):70–80.
33. Zhao Z, Ding H, Lin ZB, et al. Relationship between Tertiary Lymphoid structure and the prognosis and clinicopathologic characteristics in solid tumors. Int J Med Sci. 2021;18(11):2327–38.
34. Trajkovski G, Ognjenovic L, Karadzov Z, et al. Tertiary lymphoid structures in colorectal cancers and their prognostic value. Open Access Maced J Med Sci. 2018;6(10):1824–8.
35. Di Caro G, Bergomas F, Grizzi F, et al. Occurrence of tertiary lymphoid tissue is associated with T-cell infiltration and predicts better prognosis in early-stage colorectal cancers. Clin Cancer Res. 2014;20(8):2147–58.
36. Drayton DL, Liao S, Mounzer RH, Ruddle NH. Lymphoid organ development: from ontogeny to neogenesis. Nat Immunol. 2006;7(4):344–53.
37. Hänninen UA, Katainen R, Tanskanen T, et al. Exome-wide somatic mutation characterization of small bowel adenocarcinoma. PLoS Genet. 2018;14(3):e1007200.
38. Schrock AB, Devoe CE, McWilliams R, et al. Genomic profiling of Small-Bowel Adenocarcinoma. JAMA Oncol. 2017;3(11):1546–53.
39. Pedersen P K, Smyrk T C, Harrington S, et al. Programmed death-ligand 1 (PD-L1) expression in small bowel adenocarcinomas (SBA). Meeting Abstract. 2015;2015 ASCO Annual Meeting I GASTROINTESTINAL COLORECTAL CANCER:3619–3619.
40. Giuffrida P, Arpa G, Grillo F, et al. PD-L1 in small bowel adenocarcinoma is associated with etiology and tumor-infiltrating lymphocytes, in addition to microsatellite instability. Mod Pathol. 2020;33(7):1398–409.
41. Le DT, Uram JN, Wang H, et al. PD-1 blockade in tumors with Mismatch-Repair Deficiency. N Engl J Med. 2015;372(26):2509–20.
42. Diaz LA, Uram JN, Wang H, et al. American Society of Clinical Oncology Programmed death-1 blockade in mismatch repair deficient cancer independent of tumor histology. J Clin Oncol. 2016;34:3003.

43. Pedersen KS, Foster NR, Overman MJ, et al. ZEBRA: a Multicenter Phase II study of Pembrolizumab in patients with Advanced Small-Bowel Adenocarcinoma. Clin Cancer Res. 2021;27(13):3641–8.
44. Jun SY, Kim M, Jin Gu M, et al. Clinicopathologic and prognostic associations of KRAS and BRAF mutations in small intestinal adenocarcinoma. Mod Pathol. 2016;29(4):402–15.

Publisher's note